SciEn
Journal of Engineering Advancements Vol. 06(01) 2025, pp 1-10 https://doi.org/10.38032/jea.2025.01.001

An Experimental Study on Mechanical Properties of Stir Casted Hybrid Al Metal Matrix Composite Reinforced with Al_2O_3 and TiO_2

Md. Imtiaj Hossain, Minhaz Ahmed, Tafsirul Hassan*

Department of Mechanical Engineering, Chittagong University of Engineering & Technology, Chattogram-4349, Bangladesh

Received: October 14, 2024, Revised: December 20, 2024, Accepted: January 31, 2025, Available Online: March 04, 2025

ABSTRACT

This study investigates the impact of incorporating aluminum oxide (Al_2O_3) and titanium dioxide (TiO_2) into an aluminum matrix. The primary objectives of this research were to create composite materials with a high strength-to-weight ratio and to assess their mechanical properties. The experiment involved the homogenous dispersion of 99.9% pure aluminum powder with Al_2O_3 and TiO_2 reinforcements. Three samples were produced by the stir casting method, utilizing finely ground aluminum powder mixed with an equal proportion of Al_2O_3 and TiO_2 (2.5% Al_2O_3 + 2.5% TiO_2, 5% Al_2O_3 + 5% TiO_2, 7.5% Al_2O_3 + 7.5% TiO_2). The morphological distribution of reinforcements was determined through structural analysis utilizing a scanning electron microscope (SEM). Tests were undertaken to examine the mechanical qualities of hardness, tensile strength and impact strength. The addition of reinforcement to the aluminum matrix leads to a reduction in hardness. The highest tensile strength observed in the sample reinforced with a combination of 5% Al_2O_3 and 5% TiO_2. Conversely, the incorporation of reinforcements was observed to enhance the impact strength. The current hybrid aluminum metal matrix composite is considered valuable for diverse engineering applications that require a high strength-to-weight ratio.

Keywords: Metal matrix composite, Aluminum, Stir casting, Microstructure, Mechanical properties.

1 Introduction

Metal matrix composites (MMCs) are advanced materials made of a metal matrix reinforced with organic, ceramic and metallic components. MMCs are materials with better mechanical properties than their components. Currently, MMCs are available for use in Engineering applications in a range of forms. Most sectors, including electronics, defense, automotive and aviation, employ MMCs extensively. The discovery of MMCs has opened up a new line of inquiry into material science and engineering. Combining two or more insoluble elements that collectively possess better properties than any of the parts alone yields a composite material. When compared to traditional materials like steel, composite materials are lighter and more robust [1]. Two phases of composite materials are the matrix and the reinforcing phase. The constituents of composite materials are called reinforcements, and they typically consist of a matrix, a continuous phase and one or more discontinuous phases. The matrix keeps the reinforcement in place to achieve the desired shape, even if it enhances the matrix's overall properties [2]. Aluminum matrix composites (AMCs), are highly suited materials for many applications due to their robust physical and mechanical properties. Utilizing reinforcements improves the stiffness and particular durability, wear, creep, and fatigue properties of the metallic matrix compared to conventional Engineering materials [3]. Aluminum and its alloys have drawn the most interest as the base metal for metal matrix composites. Aluminum MMCs are frequently used in automobiles, aerospace, and several other industries. When operating at the designated temperature, the reinforcements must be both stable and non-reactive. Silicon carbide and aluminum oxide are the most often used reinforcing materials [4].

Al6061-Al_2O_3 composites containing 5 wt.% tiny Al_2O_3 particles were prepared by V. Balaraj et al. [5], and scanning electron microscopy (SEM) verified that the Al_2O_3 particles were evenly distributed throughout the matrix. Comparing the synthetic composites to the unreinforced Al6061 alloy, the former showed improved hardness, tensile strength, and impact strength. SEM investigation revealed little porosity in the matrix, although localized strain caused tiny voids to appear on the composites' fracture surfaces. Sajjadi et al. [6] employed a three-step mixing technique to fabricate materials containing 5 wt.% micron-sized and 3 wt.% nano-sized Al_2O_3 reinforcement. This was done to enhance the wetting and dispersion properties inside an aluminum alloy matrix. As the wt.% of Al_2O_3 rose, the hardness, porosity, and compressive strength also increased. Krishna et al. [7] have attempted to prepare and compare the mechanical properties of Al6061-SiC and Al6061-SiC/Graphite hybrid composites using the stir casting method. The composites have undergone microstructural investigations to describe them, with reinforcement varying between 5 and 15 wt.%. Although actual densities were lower than predicted theoretically, uniform particle dispersion with some clumping and higher tensile strength was found. Saravanan et al. [8] have explored the reinforcement of AlSi10Mg alloy with rice husk ash (RHA) to develop cost-effective metal matrix composites. It has been demonstrated that adding RHA to the composite at different weight percentages (3%, 6%, 9%, and 12%) improves its mechanical characteristics. SEM analysis has verified that the RHA particles are distributed evenly. Increased RHA content has been shown to improve tensile strength, compressive strength, and hardness, indicating its potential as a reinforcing agent. A study conducted by Ahmadifard et al. [9] focused on the manufacturing and analysis of a hybrid surface nanocomposite consisting of A5083, Al_2O_3 and TiO_2. This composite was produced using friction stir processing (FSP). The findings indicated that a combination of 25% Al_2O_3 and 75% TiO_2 yielded

*Corresponding Author Email Address: minhaz@cuet.ac.bd Published by: SciEn Publishing Group

materials with the highest tensile strength of 350 MPa and a microhardness rating of 158 HV. Utilizing in-situ Al-based MMCs generated from the Al–10 wt.% TiO_2 and Al–10 wt.% TiO_2-1.5 wt.% C systems. Peng Yu et al. [10] carried out another series of tests utilizing hot isostatic pressing (HIP) at 1000 °C and 100 MPa. Carbon's (C) inclusion aided in the intermetallic plates' elimination. The Al–10 wt.% TiO_2-1.5 wt.% C composite showed considerably better strength and strain-at-break compared to its Al–10 wt.% TiO_2 counterpart, according to three-point bending tests. The stir casting technique was effectively employed to fabricate a MMC reinforced with aluminum and a hybrid of Al_2O_3 and carbon. The results stated that there was no chemical interaction between the reinforcing components, carbon, Al_2O_3, and the aluminum matrix. The composite density decreased as the reinforcement concentration increased, reaching a minimum density of 2.04 gm/cm^3 in the AlAlOC05 specimen. The addition of carbon to the aluminum matrix resulted in a decrease in density, making it suitable for lightweight applications. According to Bandil et al. [11], the SEM microstructure investigation showed that SiC and Si alloying element particles are evenly distributed throughout the Al matrix. The reinforcing particles and matrix material did not interact, according to EDX analysis, while fabrication-related ambient oxygen trapping led to the appearance of weak oxide peaks. The density decreased as the amount of SiC in the Al matrix composites increased. The composites' hardness increased with the addition of SiC particles, reaching its maximum hardness at 15% reinforcement [12]. MMCs were characterized by Lokesh et al. using an Al6063 matrix to which different quantities of Cu and TiO_2 particles were added. With an increase in the weight percentage of Cu reinforcement, there was a little elevation in the hardness of the composites. However, when the weight percentage of reinforcement increased, the ductility of the composites decreased [13].

Muna and Jabbar [14] studied the Al-12 wt.% Si matrix composites reinforced with a hybrid addition of 2, 4 and 6 wt.% nanoparticles of Al_2O_3 and TiO_2 that exhibit dry sliding wear behavior. With varied loads and sliding periods, dry sliding wear experiments were performed and the worn surface micrographs were examined using SEM to examine wear traces and debris morphology. According to the findings, when compared to other nanocomposites, the nanocomposite containing 6 wt.% (Al_2O_3 + TiO_2) nanoparticles had the maximum hardness. Furthermore, the nanocomposites demonstrated a lower wear rate, indicating improved wear resistance compared to the base alloy under similar conditions. Naseem et al. [15] studied wear behavior, Vickers hardness, and wear data optimization for hybrid MMCs made of pure aluminum and Al-Al_2O_3-TiO_2. In the Al-Al_2O_3-TiO_2 hybrid composite, Vickers hardness rose as reinforcement proportion increased. The findings of the Analysis of Variance (ANOVA) showed that the wear rate of the hybrid composites was affected differently by both load and reinforcement. Adhesive wear predominated at lower reinforcement percentages, but abrasive wear was more common at higher reinforcement percentages, according to SEM inspection of the worn surfaces. El Mahallawi et al. [16] employed rheo-casting and included Al_2O_3/TiO_2 nanoparticles into the Al-Si slurry to produce hypereutectic aluminum-silicon samples (A390). The inclusion of nanoparticles and mechanical stirring resulted in an increase in the microhardness, hardness, and wear resistance of the A390 alloys. The addition of nanoparticles resulted in a reduction in the average size of the Si particles and an increase in hardness. The study demonstrated that the incorporation of Al_2O_3/TiO_2 nanoparticles into hypereutectic aluminum alloys yielded favorable effects. Hamid et al. [17] studied cast in situ Al(Ti)-Al_2O_3-TiO_2 composites, which are formed by dispersing TiO_2 particles in molten aluminum. Different sliding speeds under constant load and normal loads were used for wear experiments. Under identical sliding circumstances, cast in situ composites had considerably lower cumulative volume reduction and wear rates than cast commercial aluminum or cast unreinforced Al-Ti base alloys. Porosity reduced wear resistance, sometimes overshadowing reinforcing particles. Zhang et al. [18] conducted another experiment employing a mix of Al and TiO_2 powders in multiple pass friction stir processing (FSP) to manufacture in situ Al composites. The experiment was guided by thermodynamic analysis. The in-situ nanocomposites exhibited a reasonable equilibrium between strength and ductility during tensile testing and demonstrated a significant inclination towards work hardening. By using SEM, Shuvho et al. [19] exposed plowing, micro-wear, micro-cracks, fractures, voids, and particle pull-out on the surface of the Al_2O_3, SiC, and TiO_2 MMC. According to the topographical and textural analysis results, the Al6063 matrix has an evenly distributed dispersion of Al_2O_3, SiC, and TiO_2. This study demonstrates that the mechanical characteristics of the alloy, such as its hardness, tensile strength, and yield strength, are greater than those of pure Al6063 metals and increase with increasing SiC. Also, various functional groups were identified, such as O-H, C-H, CN, and -OH. El-Mahallawi et al. [20] conducted a study to explore a novel method of enhancing the characteristics of cast aluminum alloys. The analysis included introducing nanoparticles of ZrO_2, TiO_2, and Al_2O_3 into the A356 aluminum cast alloy. Analysis of the microstructure and fracture surface showed nanoparticles' existence, leading to grain morphology alterations and improved mechanical characteristics, including strength, elongation, and hardness. The incorporation of nanoparticles did not provide a substantial enhancement in the wear resistance of the hypo-eutectic A356 alloy and increasing percentages of nanoparticles resulted in a decline in performance.

Li et al. [21] effectively used FSP to create surface composites of copper matrix supplemented with Al_2O_3/TiO_2 particles. The thickness of the composite layer after undergoing three passes of processing was about 2200 µm. The addition of Al_2O_3/TiO_2 particles enhanced the hardness and thermal stability of the composites and the fracture analysis demonstrated a combination of fracture patterns, with the particles being effectively enveloped by the substrate. Ni-based alloy composite coatings were produced using the plasma spray process, using nanostructured Al_2O_3-40%TiO_2 ceramic particles as reinforcement. The findings indicate that the composite coatings mostly include γ-Ni, α-Al_2O_3, γ-Al_2O_3, and rutile-TiO_2. These coatings demonstrate reduced friction coefficients and wear losses compared to Ni-based alloy coatings at various loads and speeds. Due to the escalating contact stress over the elastic threshold, it undergoes a transition to abrasive wear, micro-brittle fracture wear, and multi-plastic deformation wear. Higher velocities lead to a 13.8% drop in the average friction coefficient and a 36.5% reduction in wear loss compared to the coating made of Ni-based alloy [22]. Nayak et al. [23] highlighted the significance of using nanofillers (Al_2O_3 and TiO_2) in glass fiber-reinforced polymer composites to observe the effect on the variation of interlaminar shear strength (ILSS). The research used SEM to examine the fracture surfaces and assess the influence of crosshead speed (CS) on the testing process.

Introducing several nanofillers resulted in higher values of ILSS and shear strain when compared to the control composites.

Jamwal et al. [24] examined the influence of SiC-graphite reinforcement on the properties of pure copper, which was fabricated using the stir-casting technique. The microstructure analysis showed a uniform distribution of SiC-graphite throughout the material. Graphite decreased hardness and density, which makes it well-suited for lightweight applications. The incorporation of SiC-graphite improves the wear resistance, exhibiting the most advantageous corrosion resistance. Paulraj et al. [25] reinforced aluminum with varying percentages of nano TiO_2, micro SiC, and B_4C respectively using a stir casting process. During manufacturing, the reinforcements were swirling at 600 rpm and heated to 750°C. Tensile strength increased from 0.5% to 1% upon the addition of TiO_2, however, elongation and impact strength decreased as the volume (%) of nano TiO_2 increased. Wear, abrasion, and friction resistance were all enhanced by combining 1% TiO_2, 10% SiC, and 10% B_4C. Toughness was increased and mass loss was decreased because of the high density. Kanthavel et al. [26] conducted a study on the three kinds of Aluminum hybrid composites that were created using powder metallurgy. The wear and friction characteristics of the three examined combinations, namely Al + 5% Al_2O_3, Al + 5% Al_2O_3 + 5% MoS_2 and Al + 5% Al_2O_3 + 10% MoS_2, were shown to be dependent on the proportion of MoS_2. The hybrid composite consisting of Al + 5% Al_2O_3 + 5% MoS_2 exhibits the lowest level of wear. The investigation indicates that including an additional 10% MoS_2 into the composite does not contribute to enhancing its tribological characteristics. Luo et al. [27] studied the alteration of KH560, an epoxy-functional silane, after hydrothermally synthesizing spherical Al_2O_3/TiO_2 nanocomposites. The average diameter of the modified nanoparticles was 75 nm, and they exhibited good dispersion stability in lubricating oil. Through four-ball and thrust-ring testing, it was shown that the addition of modified Al_2O_3/TiO_2 nanocomposites at an optimal concentration of 0.1 wt.% dramatically reduced friction coefficients and increased anti-wear performance. The nanocomposites converted sliding friction into rolling friction by forming a shielding covering on the rubbing surfaces during friction. Ylma et al. [28] produced Al_2O_3-TiO_2 plasma sprayed coatings of different compositions on an AISI 304L stainless steel substrate. Investigations were conducted to determine how the addition of TiO_2 affected the coatings. It was evident from the traditional evaluation of the experimental results that a higher TiO_2 concentration reduced microhardness values and enhanced fracture toughness. The microhardness of the alumina coating was dramatically reduced by the addition of TiO_2, which increased toughness. Aluminum, magnesium, and graphite have lower densities than copper, as shown by Oddone et al. [29]. They obtain four times greater heat conductivity than copper because of their low density. An Aluminum-3003 alloy metal matrix, reinforced with single-walled carbon nanotubes (CNTs) and titanium carbide (TiC), was produced using the stir casting technique. It has been observed that when the number of reinforcements increases, particles are more even. The density of composites decreases as a result of the volatile nature of the reinforcing particles. Reinforcement determines composite hardness and composites wear less as load lowers and reinforcing rises [30].

It seems that not enough research has been done on the microstructure analysis of hybrid AMMCs. There hasn't been enough thorough research done on the mechanical characterization of hybrid AMMCs and the effects of various reinforcing arrangements, manufacturing techniques on the mechanical characteristics of hybrid AMMCs. This study has been conducted to close the information gap about the mechanical properties of a stir-casted hybrid AMMC reinforced with Al_2O_3 and TiO_2. This research aims to examine the structural and mechanical characteristics of a hybrid composite material. A hybrid composite, consisting of Al_2O_3 and TiO_2, has been fabricated via stir casting. This involves analyzing many aspects of the final composite material, such as its microstructure, hardness, impact strength, and tensile strength. To further enhance this investigation, modern manufacturing techniques like as infiltration, plasma sintering, hot pressing, and powder metallurgy may be used.

2 Materials and Method

2.1 Stir Casting Method

The first stage in producing an Al-Al_2O_3-TiO_2 matrix by the stir casting method entails obtaining high-purity sample powders of Al, Al_2O_3, and TiO_2 from an accredited vendor. The reinforcements utilized consist of Al_2O_3 powder with a purity of 96% and TiO_2 powder with a purity of 99%. The stir casting system used a silicon carbide stirrer, a graphite crucible, an electrical furnace, a temperature controller, and a cylindrical die composed of high chrome high carbon steel. To fabricate the samples, the powders are measured based on the specified wt.% chosen. Three samples with varied weight proportions have been created throughout the production process. The weights of the powders vary depending on the individual tests being performed. Al_2O_3 and TiO_2 are used as the reinforcing material, with aluminum serving as the matrix material in this case. The final specimen is prepared using a total of 600 g of powder. A quantity of 200 g has been used for each combination. In this case, 190 g of Al is combined with 5 g each of TiO_2 and Al_2O_3, resulting in a composition of 95% Al, 2.5% TiO_2, and 2.5% Al_2O_3. The remaining two combinations have been acquired in the same way. To reduce the moisture content, the crucible has spent 30 min in the electrical furnace at 510 °C. Then, to remove moisture and stop oxidation, reinforcement materials such as Al_2O_3 and TiO_2 have been put in the crucible and held within the furnace for 45 min at 540 °C. In this procedure, the Aluminum powder is not warmed to avoid the oxidation of aluminum.

To achieve the needed criteria, the Al matrix has been broken up into smaller pieces and weighed appropriately using an automated weighing scale. The Al matrix was then been added to the crucible before being put inside the furnace. The temperature of the furnace has been raised progressively to 920 °C and then held there for 30 min. The Al matrix has then melted and gradually changed into a molten state after a 30-min period. Then, the warmed reinforcements were placed in the furnace and stirred for 30 min before being heated to 940 °C for 8 min. The fusion of the matrix and reinforcing components has been successfully achieved in the furnace via the process of melting. After the particles were completely liquefied, a manual stirring method was used using a hand stirrer. A vortex was generated in the molten aluminum by rotating the stirrer for a duration of 10 min. Once the metal has been melted, it is next poured into molds to get the desired form of the specimen. The final samples have been produced after the molds solidified. Once the composites have fully hardened, further techniques such as thread cutting, taper turning, grinding and slot cutting must be performed. The tensile specimens were fabricated using thread-cutting and taper

turning techniques. Slots were added to the impact specimens. Final specimens were produced after completing all the tasks outlined in Table 1.

Table 1 Nomenclature of Al-Al_2O_3-TiO_2 hybrid composite samples.

Sample	Al (wt.%)	Al_2O_3 (wt.%)	TiO_2 (wt.%)
Sample (i)	95%	2.5%	2.5%
Sample (ii)	90%	5%	5%
Sample (iii)	85%	7.5%	7.5%

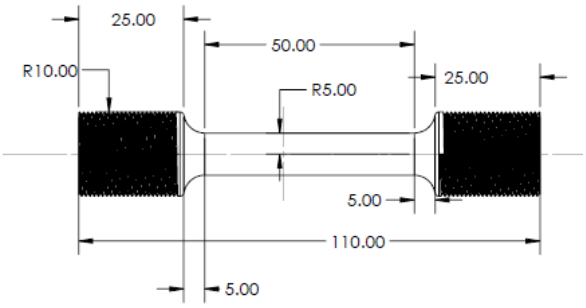

Fig. 1 Specimen for tensile test (All dimensions are in mm).

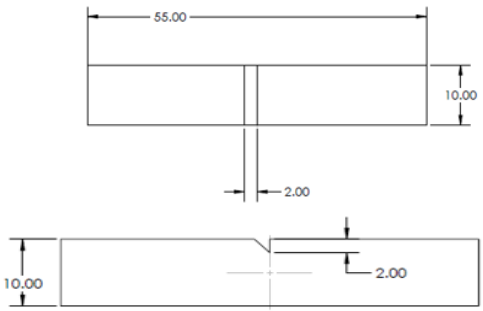

Fig. 2 Specimen for impact test (All dimensions are in mm).

Fig. 3 Final specimens for a) Hardness test, b) Impact test, and c) Tensile test.

Fig. 4 Final specimens after testing for a) Hardness test, b) Impact test, and c) Tensile test.

2.2 Characterization

The specimens were prepared using a SEM at magnifications of 500x, 1100x, 1500x, and 2000x for morphological analysis. Preparation of samples for various tests, including SEM and energy dispersive spectroscopy (EDS), involves the process of polishing. The samples were polished properly using emery paper of grades starting from 280, 360, 500, and 1000 for 20 min and after that, polishing of the samples was done with alumina gel for 20min.

To comprehend the mechanical properties of metallic materials, including their tensile strength, yield strength, and ultimate tensile strength, it is necessary to conduct tensile testing. The experimental data was collected and used to generate a stress-strain curve to analyze the tensile behavior of the specimens. A universal testing machine (UTM) was utilized to quantify the tensile strength. The dimensions of the tensile test specimen, as specified by the ASTM (American Society for Testing and Materials), are illustrated in Fig. 1. Three samples were prepared for tensile testing, and each sample was tested sequentially under identical conditions. The UTM employed was a manual device, where the applied load was controlled via a hand-operated lever or valve. The load values were displayed on a gauge, while displacement data were manually recorded from another gauge. During the test, the loading process was manually controlled by adjusting a mechanical lever to apply force to the specimens. While recording the data, there was a slight decrease in force immediately after reaching the maximum force (approximately 100 N for Sample (i)), just before the specimen fractured. From the recorded data, the maximum force (F) was used to calculate UTS, and the breaking force was used to calculate tensile strength. The cross-sectional area (A) was calculated using the initial diameter (D) of the samples. Calculations for UTS, tensile stress, and cross-sectional area were performed using the following formulas:

$$\sigma = \frac{F}{A} \tag{1}$$

$$A = \frac{\pi}{4} D^2 \tag{2}$$

The Brinell hardness tester was employed to ascertain the hardness of the composites with varying ratios. The Brinell hardness test involves applying a constant force of 10 kN for a duration of 10 s by placing a tungsten carbide ball with a diameter of 10 mm on the flat surface of a workpiece. The indentation diameter is determined by measuring the horizontal and vertical axis radii of the hole formed, and then calculating their average using a digital slide caliper. Charpy V-notch test was employed to quantify the energy absorbed by the samples before fracture. The purpose of loading the specimens into the machine was to fracture them ultimately. The impact value was promptly derived from the measurement of impact strength utilizing a digital impact tester apparatus. The dimensions of the Charpy test specimen for measuring impact strength are also depicted in Fig. 2.

3 Results and Discussions

3.1 Microstructure Analysis

3.1.1 Distribution of Reinforcements

The microstructure analysis was employed to investigate the morphological behavior of the composite material that was produced. Fig. 5 displays the SEM images of the sample (ii) consisting of 90% Al, 5% Al_2O_3, and 5% TiO_2. The images were captured at magnifications of 500x, 1100x, and 2000x, respectively. Due to its non-conductive nature, Al_2O_3 tends to form clusters in certain areas and appear white. The regions in the image showing such clustering and whiteness are Al_2O_3. On the other hand, TiO_2 has some recognizable visual traits, such as rounded shapes and bright contrast. In the SEM image, we identified and marked certain areas based on these characteristics as potential TiO_2.

The distribution of reinforcements throughout the Al matrix is found to be uniform. This guarantees that the highest possible amount of reinforcement particles in the aluminum matrix is dispersed homogeneously due to the insoluble nature of the Al_2O_3 and TiO_2 particles.

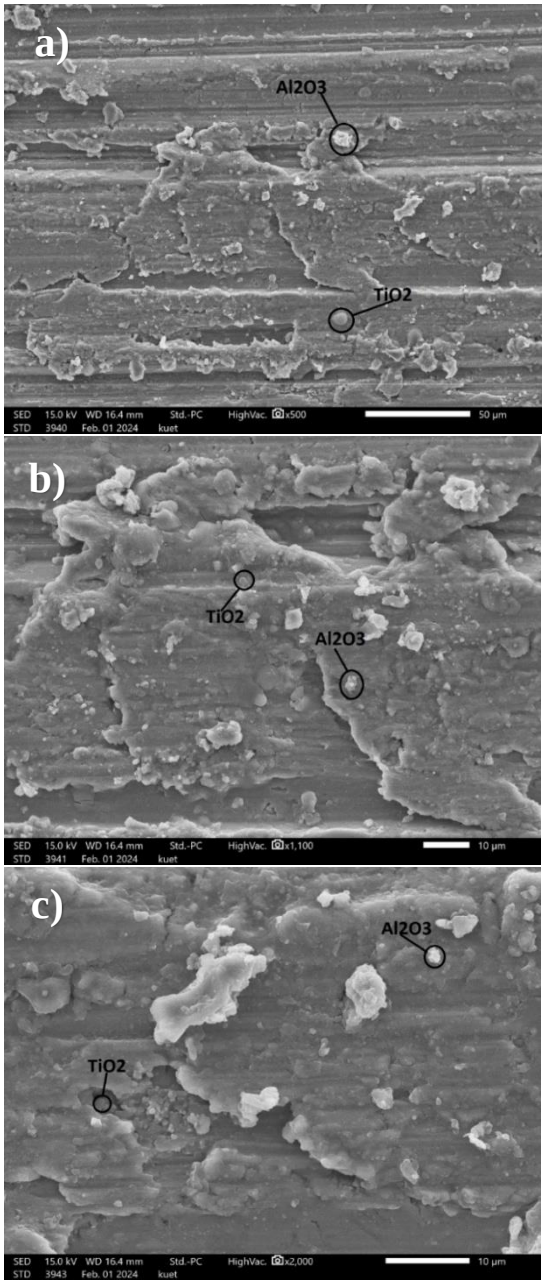

Fig. 5 SEM micrograph of sample (ii) at a) 500x magnification, b) 1100x magnification, and c) 2000x magnification.

In the stir casting process, it is clearly observed that reinforcement particles get collected during the stirring process. It is a difficult task to properly mix and distribute Al_2O_3 and TiO_2 inside the aluminum matrix. It is possible to achieve a homogeneous microstructure with reduced reinforcing concentrations. Particle agglomeration occurs during the stirring process as a result of the substantial density variations between the matrix and reinforcement phases, which make it more difficult to achieve equal distribution at higher concentrations. Also, there is a high chance of getting a non-uniform distribution of reinforcements because of an improper stirring process.

3.1.2 Grain Size Distribution

We examined the grain size distribution of sample (ii) using Image J and Origin Pro software. Fig. 6 depicts SEM micrographs of the sample at 1500x and 2000x magnifications, respectively, showcasing a uniform distribution of grains within the Al matrix.

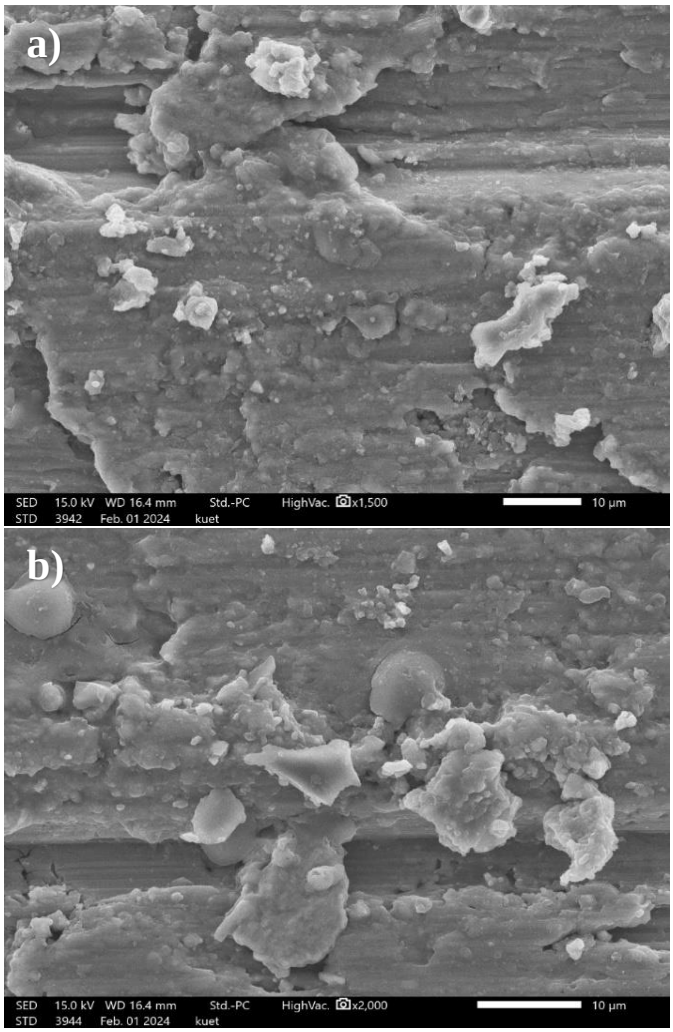

Fig. 6 SEM micrograph of sample (ii) at a) 1500x magnification, b) 2000x magnification.

Significantly, the sample exhibits a notable abundance of granular particles of different sizes, as depicted in Fig. 6. The distribution curve depicted in Fig. 7 represents a normal distribution curve with an average grain diameter of 1.18 microns and a standard deviation of 0.41909. Approximately 30% of the grains in the sample (ii) have diameters ranging from 1 to 1.25 microns, whereas the remaining 70% have sizes that vary.

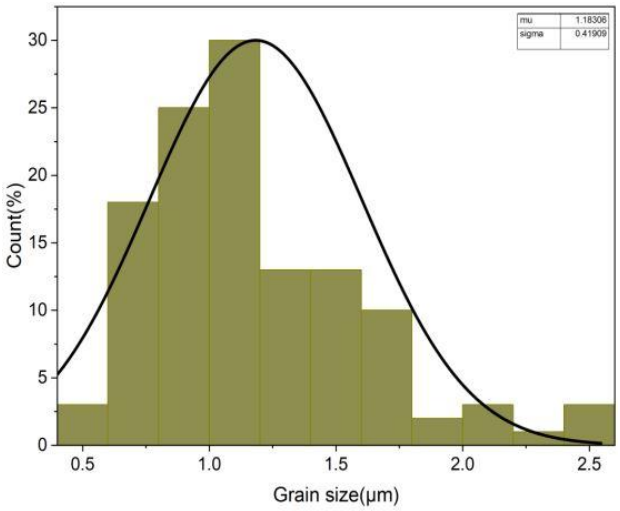

Fig. 7 Normal distribution curve of sample (ii)

The analysis reveals a significant presence of diverse grain sizes, highlighting the homogeneous nature of the sample. These findings underscore the complexity of the material structure and emphasize the importance of accurately characterizing grain size distribution for understanding its properties and potential applications. The use of advanced imaging and analytical tools such as Image J and Origin Pro facilitates precise examination, enabling insights into the microstructural features critical for material performance evaluation and optimization.

3.1.3 Energy Dispersive Spectroscopy

The EDS of the sample (ii) (Al 90% + Al_2O_3 5% + TiO_2 5%) is displayed below in Fig. 8. Al has the highest peak in this sample out of all of them. The elements with the lowest peak in the specimen are C, Sn, Cu, Mg, and Au, all of which are present in extremely small amounts. Among all of them, Sn has the lowest peak. It is discovered that Sn is integrated amongst O, C, Sn, Cu, Mg, and Au and has no weight percentage in the composite. In addition to having the effect of reducing ambient gases during the stirrer, applying vacuum to the molten matrix and reinforcement mixture also tends to dissolve, entrap, and adsorb gases out of the melt during mixing. Sample (ii) has very little oxygen in it after manufacture because the composite is well-insulated from the environment during the process.

We observed peaks for Al and O, confirming the presence of Al_2O_3 in the sample. However, the EDS analysis did not show a Ti peak, which could be due to several reasons, such as the agglomeration of TiO_2 particles, surface preparation issues, or peak overlap. Nonetheless, in the next sections, we will observe a decreasing trend in hardness and an increasing trend in impact strength with the addition of TiO_2 reinforcement in the matrix, attributed to the soft and low-density nature of Ti.

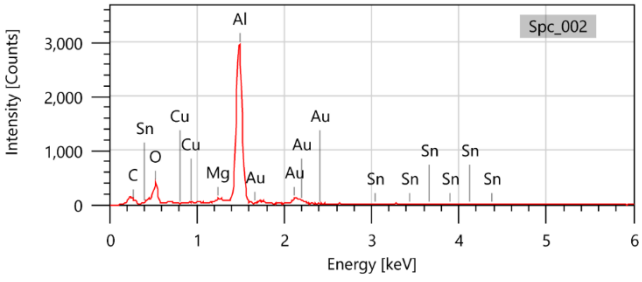

Fig. 8 EDS spectrum of sample (ii).

3.2 Hardness Number

Fig. 9 displays the hardness of various composite specimens. From [31], the hardness of Al 6351 is 109 BHN. Significantly, when the amount of reinforcement increases, the hardness of the composite decreases. Sample (iii) demonstrates the lowest recorded hardness value of 74.84 BHN, mostly attributed to its elevated titanium concentration. In contrast, sample (i) demonstrates the maximum recorded hardness value of 96.33 BHN due to its relatively lower titanium content. Fig. 9 serves to visually represent the comparative Brinell Hardness Numbers of the sample composites, offering insights into the discernible differences in hardness relative to varying titanium concentrations.

The differences in hardness values across the samples highlight the direct influence of titanium concentration on the hardness of the composite. The greater concentration of reinforcement, which is probably the result of reinforcement particle agglomeration and a decrease in matrix wettability, is responsible for the composite's decreased hardness. The agglomeration of reinforcement particles reduces their exposed surface area, affecting the wettability of the aluminum matrix. These particle clusters disrupt uniform dispersion, resulting in poor bonding and decreased wettability in certain regions. Furthermore, when the reinforcing content increases, the density of the composite drops. During mechanical testing, the presence of titanium particles produces voids that provide ideal conditions for the nucleation and development of cracks. The soft and low-density nature of titanium is the main cause of the decrease in the overall hardness of the composite material. The reduced hardness seen in composites reinforced with titanium oxide can be explained by this phenomenon. The results showed a similar pattern to what Ahamad et al. described [31].

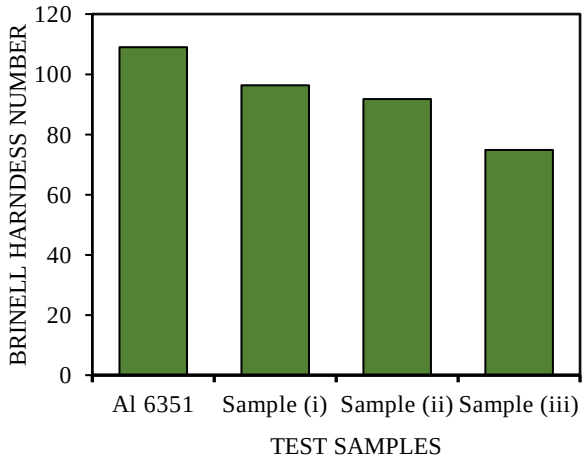

Fig. 9 Brinell Hardness Number of composite samples.

3.3 Tensile Behaviors

Tensile strength, Ultimate Tensile Strength (UTS) and Yield strength are evaluated from the load-displacement curve as well as the stress-strain curve.

3.3.1 Sample (i) Tensile Properties

For sample (i) (95% Al + 2.5% Al2O3 + 2.5% TiO2) from Fig. 10, it is observed that the peak load is 2.7 kN whereas, the displacement at peak load is 0.45 mm. The maximum strength of the specimen is represented by the peak load of the sample (i) which we can see in Fig. 11. At peak load stress-strain curve gives the value of UTS which is 34.38 MPa. Fig. 8 displays that

the initially applied load varies up to the peak point thereafter peak point decreases with increasing applied load. At the breaking point, the load diminishes to 2.6 kN with a displacement of 0.50 mm. The tensile strength at the breaking load is measured at 33.10 MPa, as depicted by the stress-strain curve. Additionally, the yield strength is determined from the stress-strain curve, yielding a value of 22 MPa. Fig. 10 for the load-displacement curve and Fig. 11 for the stress-strain curve is illustrated below.

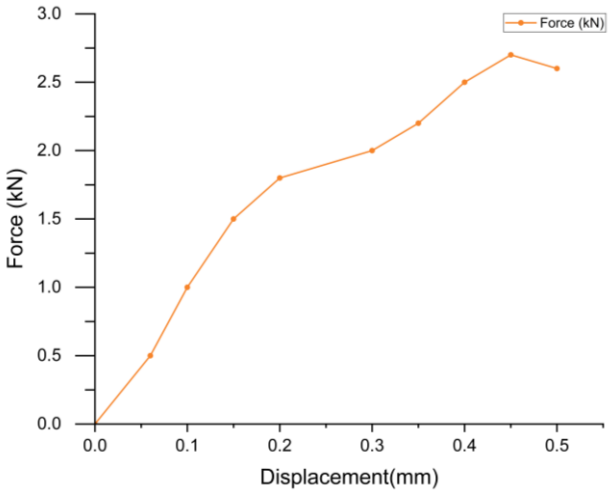

Fig. 10 Load Vs displacement curve for sample (i).

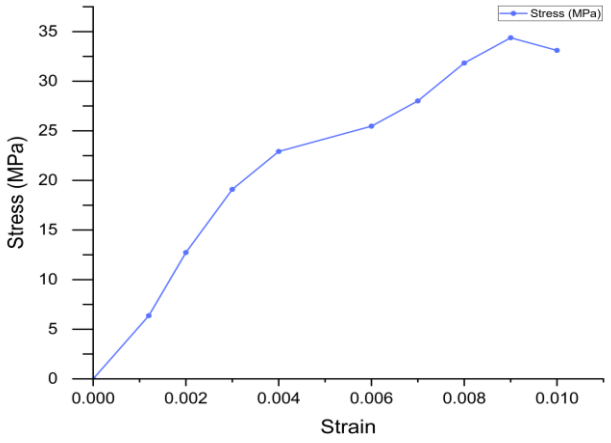

Fig. 11 Stress Vs Strain curve for sample (i).

3.3.2 Sample (ii) Tensile Properties

In Fig. 12, sample (ii) consisting of 90% Al, 5% Al2O3, and 5% TiO2, has a displacement of 0.60 mm at peak load and a peak load of 5 kN. Fig. 13 displays the stress-strain relationship for sample (ii), illustrating the tensile properties of the specimen. The stress-strain curve reaches its maximum load at a value of 63.66 MPa, which is known as the UTS. At the breaking point, the force reduces to 4.8 kN while causing a displacement of 0.65 mm. The stress-strain curve indicates that the tensile strength at the point of fracture is 61.12 MPa, whereas the yield strength is also 40 MPa.

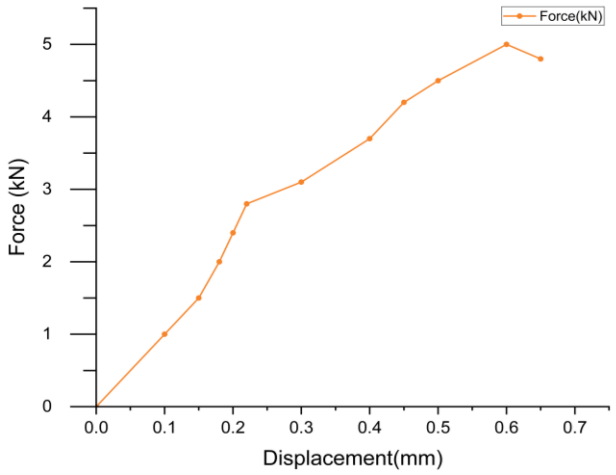

Fig. 12 Load Vs displacement curve for sample (ii).

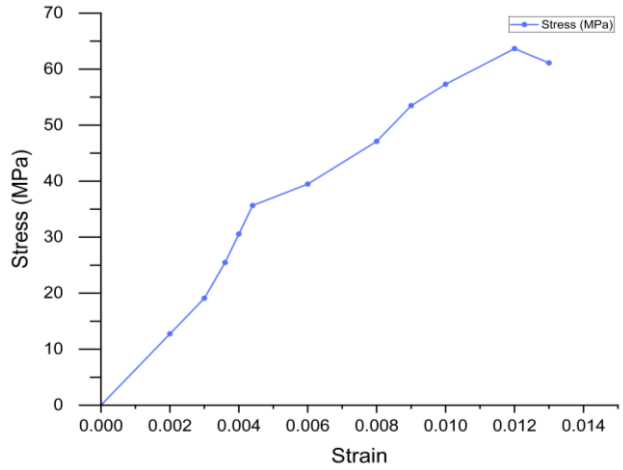

Fig. 13 Stress vs Strain curve for sample (ii).

3.3.3 Sample (iii) Tensile Properties

The peak load for sample (iii) (85% Al + 5% Al2O3 + 2.5% TiO2) in Fig. 14 is observed to be 3.5 kN, whereas the displacement at peak load is 0.50 mm. Fig. 15 shows the stress-strain curve for sample (iii). The stress-strain curve at peak load yields the UTS value of 44.56 MPa. The load decreases to 3.4 kN with a 0.55 mm displacement at the breaking point. The stress-strain curve shows that the tensile strength at the breaking load is 33.10 MPa and yield strength 24 MPa.

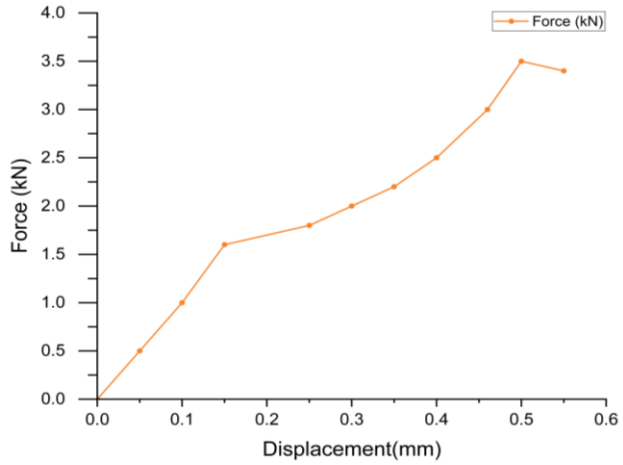

Fig. 14 Load Vs displacement curve for sample (iii).

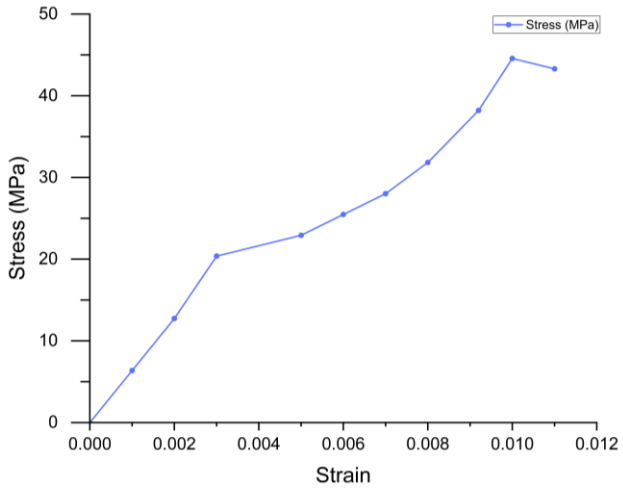

Fig. 15 Stress Vs Strain curve for sample (iii).

3.3.4 Comparative Analysis of Tensile Behaviors

Based on the analysis, it has been determined that the tensile properties of the three samples exhibit variances due to differences in reinforcement. The tensile strength, UTS, and yield strength for sample (i) are 33.10 MPa, 34.38 MPa, and 22 MPa, respectively. In sample (ii), the tensile characteristics showed a substantial increase. The tensile strength, UTS, and yield strength were measured at 61.12 MPa, 63.66 MPa, and 40 MPa, respectively. It has been observed that the tensile characteristics of the composite increase as the reinforcing percentage increased. However, in the case of sample (iii), we observed a tensile strength of 43.29 MPa, an UTS of 44.56 MPa, and a yield strength of 24 MPa. These values are lower than those of sample (ii) but higher than those of sample (i). Based on the SEM images of the sample (ii), we observed a consistent dispersion of reinforcing material throughout the matrix. This uniform distribution contributes to the sample's superior tensile capabilities compared to the other two samples. Below Table 2 shows the maximum tensile load data of the composite samples.

Table 2 Maximum tensile load data of the composite samples.

Sample no.	Diameter, D(mm)	Initial Length, L(mm)	Maximum tensile load, F(kN)
i	10	50	2.7
ii	10	50	5
iii	10	50	3.5

From the observations, it is found that on an increasing percentage of reinforcement in the Al matrix up to 10%, tensile properties increase significantly. Because up to 10% reinforcement, there is a uniform distribution of reinforcement throughout the Al matrix. But when the weight percentage of reinforcement in the Al matrix is above 10%, tensile properties decrease.

A well-dispersed composite allows for improved load transmission because of the more consistent bonding between the matrix and the reinforcing particles (Al_2O_3 and TiO_2). Nevertheless, weak interactions between the matrix and the dispersed particles may result from a heterogeneous distribution. When tensile stress is applied, poor bonding at these interfaces makes it simpler for the material to crack, which lowers the material's overall strength. Also, Particle clustering results in cavities or additional defects in the material. The material is weakened by these voids because they decrease the effective cross-sectional area that bears the tensile force. Because of internal stress concentrations, clusters themselves may serve as sites where cracks begin. The equal distribution of reinforcement, on the other hand, facilitates effective load transmission from the matrix material to the reinforcement, increasing the composite's tensile strength. So, because of the non-uniformity and the influence of reinforcing particle segregation in tensile test specimen, it has been shown that an increase in Al_2O_3 and TiO_2 particles above 10% lowers tensile strength. Fig. 16 illustrates the comparative tensile behavior of the samples.

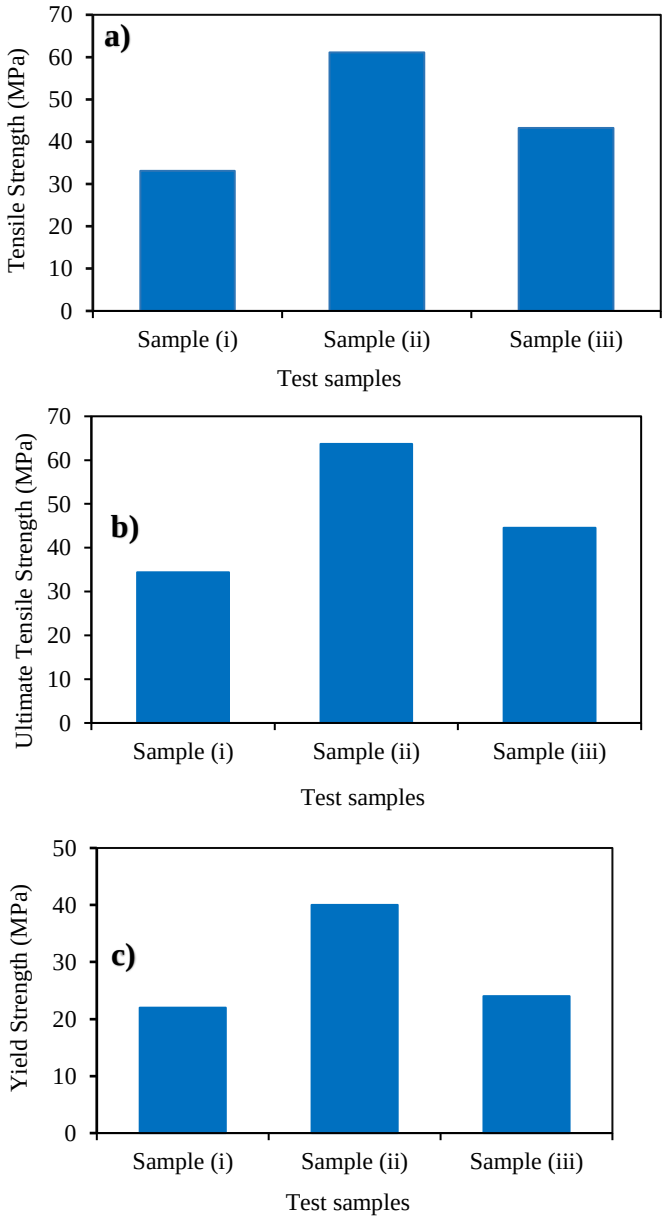

Fig. 16 a) Tensile strength, b) UTS, and c) Yield strength of composite samples.

3.4 Impact strength

The Charpy impact test was done where the V-notch specimens of the composites were used. The test was done by a digital impact tester with a simple pendulum hammer. Ahamad

et al. found that the impact strength of Al 6351 is 29 J [31]. Fig. 17 illustrates the impact strength of the samples. The impact strength of sample (i) is measured to be 32.7 J, while the impact strength of sample (ii) is somewhat higher at 41.8 J. However, in the sample (iii), we observed a substantial and notable increase in impact strength, measuring 54.5 J. It is observed that the hybrid composite specimen's impact strength is contingent upon the percentage of reinforcement present.

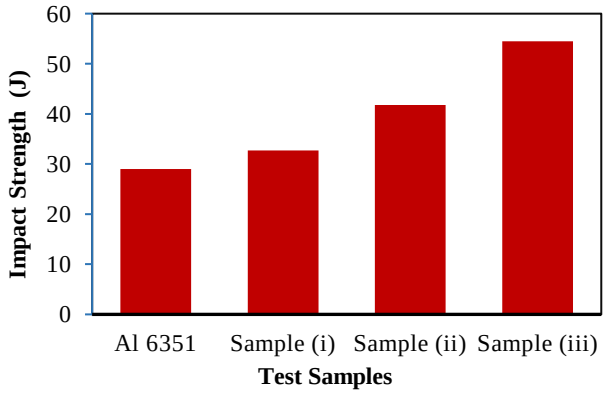

Fig. 17 Impact Strength of composite samples.

Research has shown that the addition of reinforcement to the aluminum matrix leads to an increase in the impact strength of the composite. As the amount of reinforcement rises, the surface of the composite becomes softer, and its ability to withstand impact increases, allowing it to tolerate higher forces before breaking. Therefore, sample (iii) containing 15% reinforcement has the highest impact energy. The findings displayed a pattern that was comparable to that reported by Ahamad et al. [31].

4 Conclusion

The fabrication of stir-casted hybrid AMMCs augmented with Al_2O_3 and TiO_2 was the main emphasis of this research. Stir casting has been used to combine the fine aluminum powder with different combinations of Al_2O_3 and TiO_2(2.5% Al_2O_3+2.5% TiO_2, 5%Al_2O_3+5% TiO_2, 7.5% Al_2O_3+7.5% TiO_2). And also explored mechanical characteristics such as tensile strength, hardness, impact strength and microstructure analysis using SEM. The concluded remarks of the present experimental study are as follows:

The stir casting technique was successfully employed to make these composites, resulting in enhanced mechanical properties such as increased tensile strength and impact strength. The impact of varying the concentration of reinforcement on these parameters has been investigated by altering the content of Al_2O_3 and TiO_2.

The SEM micrographs reveal a consistent dispersion of reinforcement throughout the aluminum matrix, as well as the grain size distribution of the composite. Approximately 30% of the grains have a size between 1-1.25 microns. The average diameter of the grain is 1.18 microns. It has shown the uniform distribution of the reinforcement in the Al matrix.

The Brinell Hardness Numbers for sample (i), sample (ii), and sample (iii) are 96.33 BHN, 91.79 BHN, and 74.84 BHN respectively. The hardness test showed that sample (iii), which had a higher reinforcement of 7.5% Al_2O_3+7.5% TiO_2, had a lower hardness compared to the other specimens. The incorporation of TiO_2 powder into the Al matrix results in a reduction in the hardness of the composite material, which is advantageous for applications requiring lightweight materials.

Sample (i), (ii), and (iii) had tensile strengths of 33.10 MPa, 61.12 MPa, and 43.29 MPa, in that order. Sample (ii) reinforced with 5% Al_2O_3 and 5% TiO_2 have the maximum value of tensile strength. Al matrix gives decreasing tensile strength when the weight percentage of reinforcements in the Al matrix is greater than 10%.

Impact strength increases with an increase in reinforcement content in the composite and the maximum impact strength is 54.5 J for the sample with reinforcement of 7.5% Al_2O_3+7.5% TiO_2. While for sample (i) and sample (ii) impact strengths are 32.7 J and 41.8 J respectively.

This study can be further improved by taking some precautions and steps. So, the following recommendation can be mentioned after conducting the experimental investigation for future researchers:

AMMC with the same composition and experimental procedure might exhibit brittle behavior in one experiment and ductile behavior in another because of temperature, microstructure variations, testing conditions and material aging. So have to be cautious during the whole fabrication process.

In order to improve mechanical properties and give better uniformity among different particles, this study can be expanded by utilizing modern manufacturing techniques such as infiltration, plasma sintering, hot pressing and powder metallurgy.

References

[1] Ramanathan, A., Krishnan, P.K. and Muraliraja, R., 2019. A review on the production of metal matrix composites through stir casting–Furnace design, properties, challenges, and research opportunities. Journal of Manufacturing processes, 42, pp.213-245.

[2] Sharma, A.K., Bhandari, R., Aherwar, A. and Rimašauskienė, R., 2020. Matrix materials used in composites: A comprehensive study. Materials Today: Proceedings, 21, pp.1559-1562.

[3] Ramnath, B.V., Elanchezhian, C., Annamalai, R.M., Aravind, S., Atreya, T.S.A., Vignesh, V. and Subramanian, C., 2014. Aluminium metal matrix composites–a review. Rev. Adv. Mater. Sci, 38(5), pp.55-60.

[4] McDanels, D.L., 1985. Analysis of stress-strain, fracture, and ductility behavior of aluminum matrix composites containing discontinuous silicon carbide reinforcement. Metallurgical transactions A, 16, pp.1105-1115.

[5] Balaraj, V., Kori, N., Nagaral, M. and Auradi, V., 2021. Microstructural evolution and mechanical characterization of micro Al2O3 particles reinforced Al6061 alloy metal composites. Materials Today: Proceedings, 47, pp.5959-5965.

[6] Sajjadi, S.A., Ezatpour, H.R. and Beygi, H., 2011. Microstructure and mechanical properties of Al–Al2O3 micro and nano composites fabricated by stir casting. Materials Science and Engineering: A, 528(29-30), pp.8765-8771.

[7] Krishna, M.V. and Xavior, A.M., 2014. An investigation on the mechanical properties of hybrid metal matrix composites. Procedia Engineering, 97, pp.918-924.

[8] Saravanan, S.D. and Kumar, M.S., 2013. Effect of mechanical properties on rice husk ash reinforced

aluminum alloy (AlSi10Mg) matrix composites. Procedia Engineering, 64, pp.1505-1513.

[9] Ahmadifard, S., Kazemi, S. and Heidarpour, A., 2018. Production and characterization of A5083–Al2O3–TiO2 hybrid surface nanocomposite by friction stir processing. Proceedings of the Institution of Mechanical Engineers, Part L: Journal of Materials: Design and Applications, 232(4), pp.287-293.

[10] Yu, P., Mei, Z. and Tjong, S.C., 2005. Structure, thermal and mechanical properties of in situ Al-based metal matrix composite reinforced with Al2O3 and TiC submicron particles. Materials Chemistry and Physics, 93(1), pp.109-116.

[11] Ahamad, N., Mohammad, A., Sadasivuni, K.K. and Gupta, P., 2020. Phase, microstructure and tensile strength of Al–Al2O3–C hybrid metal matrix composites. Proceedings of the Institution of Mechanical Engineers, Part C: Journal of Mechanical Engineering Science, 234(13), pp.2681-2693.

[12] Bandil, K., Vashisth, H., Kumar, S., Verma, L., Jamwal, A., Kumar, D., Singh, N., Sadasivuni, K.K. and Gupta, P., 2019. Microstructural, mechanical and corrosion behaviour of Al–Si alloy reinforced with SiC metal matrix composite. Journal of Composite Materials, 53(28-30), pp.4215-4223.

[13] Lokesh, N., Manoj, B., Srikanth, K., Ramanayya, P.K.V. and Rao, M.V., 2018. Mechanical characterization of stir cast Al 6063 TiO2-Cu reinforced hybrid metal matrix composites. Materials Today: Proceedings, 5(9), pp.18383-18392.

[14] Abbass, M.K. and Fouad, M.J., 2015. Wear characterization of aluminum matrix hybrid composites reinforced with nanoparticles of Al2O3 and TiO2. Journal of Materials Science and Engineering B, 5(9-10), pp.361-371.

[15] Ahamad, N., Mohammad, A., Sadasivuni, K.K. and Gupta, P., 2021. Wear, optimization and surface analysis of Al-Al2O3-TiO2 hybrid metal matrix composites. Proceedings of the institution of mechanical engineers, Part J: Journal of Engineering Tribology, 235(1), pp.93-102.

[16] El Mahallawi, I., Shash, Y., Rashad, R.M., Abdelaziz, M.H., Mayer, J. and Schwedt, A., 2014. Hardness and wear behaviour of semi-solid cast A390 alloy reinforced with Al 2 O 3 and TiO 2 nanoparticles. Arabian Journal for Science and Engineering, 39, pp.5171-5184.

[17] Hamid, A.A., Ghosh, P.K., Jain, S. and Ray, S., 2008. The influence of porosity and particles content on dry sliding wear of cast in situ Al (Ti)–Al2O3 (TiO2) composite. Wear, 265(1-2), pp.14-26.

[18] Zhang, Q., Xiao, B.L., Wang, Q.Z. and Ma, Z.Y., 2011. In situ Al3Ti and Al2O3 nanoparticles reinforced Al composites produced by friction stir processing in an Al-TiO2 system. Materials Letters, 65(13), pp.2070-2072.

[19] Shuvho, M.B.A., Chowdhury, M.A., Kchaou, M., Roy, B.K., Rahman, A. and Islam, M.A., 2020. Surface characterization and mechanical behavior of aluminum based metal matrix composite reinforced with nano Al2O3, SiC, TiO2 particles. Chemical Data Collections, 28, p.100442.

[20] El-Mahallawi, I.S., Shash, A.Y. and Amer, A.E., 2015. Nanoreinforced cast Al-Si alloys with Al2O3, TiO2 and ZrO2 nanoparticles. Metals, 5(2), pp.802-821.

[21] Li, C., Feng, X., Shen, Y. and Chen, W., 2016. Preparation of Al2O3/TiO2 particle-reinforced copper through plasma spraying and friction stir processing. Materials & Design, 90, pp.922-930.

[22] Long, H.E., Tan, Y.F., Hua, T.A.N., Zhou, C.H. and Li, G.A.O., 2013. Tribological properties of nanostructured Al2O3-40% TiO2 multiphase ceramic particles reinforced Ni-based alloy composite coatings. Transactions of Nonferrous Metals Society of China, 23(9), pp.2618-2627.

[23] Nayak, R.K., Mahato, K.K., Routara, B.C. and Ray, B.C., 2016. Evaluation of mechanical properties of Al2O3 and TiO2 nano filled enhanced glass fiber reinforced polymer composites. Journal of Applied Polymer Science, 133(47).

[24] Jamwal, A., Prakash, P., Kumar, D., Singh, N., Sadasivuni, K.K., Harshit, K., Gupta, S. and Gupta, P., 2019. Microstructure, wear and corrosion characteristics of Cu matrix reinforced SiC–graphite hybrid composites. Journal of Composite Materials, 53(18), pp.2545-2553.

[25] Paulraj, D., Jeyakumar, P.D., Rajamurugan, G. and Krishnasamy, P., 2021. Influence of nano TiO2/micro (SiC/B4C) reinforcement on the mechanical, wear and corrosion behaviour of A356 metal matrix composite. Archives of Metallurgy and Materials, 66(3), pp.871-880.

[26] Kanthavel, K., Sumesh, K.R. and Saravanakumar, P., 2016. Study of tribological properties on Al/Al2O3/MoS2 hybrid composite processed by powder metallurgy. Alexandria Engineering Journal, 55(1), pp.13-17.

[27] Luo, T., Wei, X., Zhao, H., Cai, G. and Zheng, X., 2014. Tribology properties of Al2O3/TiO2 nanocomposites as lubricant additives. Ceramics International, 40(7), pp.10103-10109.

[28] Yılmaz, R., Kurt, A.O., Demir, A. and Tatlı, Z., 2007. Effects of TiO2 on the mechanical properties of the Al2O3–TiO2 plasma sprayed coating. Journal of the European Ceramic Society, 27(2-3), pp.1319-1323.

[29] Oddone, V., Boerner, B. and Reich, S., 2017. Composites of aluminum alloy and magnesium alloy with graphite showing low thermal expansion and high specific thermal conductivity. Science and Technology of advanced MaTerialS, 18(1), pp.180-186.

[30] Nayim, S.T.I., Hasan, M.Z., Seth, P.P., Gupta, P., Thakur, S., Kumar, D. and Jamwal, A., 2020. Effect of CNT and TiC hybrid reinforcement on the micro-mechano-tribo behaviour of aluminium matrix composites. Materials Today: Proceedings, 21, pp.1421-1424.

[31] Ahamad, N., Mohammad, A., Sadasivuni, K.K. and Gupta, P., 2020. Structural and mechanical characterization of stir cast Al–Al2O3–TiO2 hybrid metal matrix composites. Journal of Composite Materials, 54(21), pp.2985-2997.